Real-time Zika risk assessment in the United States

Lauren A Castro*[,1], BA, Spencer J Fox*[,1@], BS , Xi Chen[2] MS, Kai Liu[3] MS, Steve Bellan[4] PhD, Nedialko B Dimitrov[2] PhD, Alison P Galvani[5,6] PhD, Lauren Ancel Meyers[1,7] PhD

Affiliations:

1 - Department of Integrative Biology, The University of Texas at Austin, Austin, TX, USA

2 - Graduate Program in Operations Research Industrial Engineering, The University of Texas at Austin, Austin, TX, USA

3 - Institute for Cellular and Molecular Biology, The University of Texas at Austin, Austin, TX, USA

4 - Center for Computational Biology and Bioinformatics, The University of Texas at Austin, Austin, TX, USA

5 - Center for Infectious Disease Modeling and Analysis, Yale School of Public Health, New Haven, CT, USA

6 - Department of Ecology and Evolution, Yale University, New Haven, CT, USA

7 - The Santa Fe Institute, Santa Fe, NM, USA

* contributed equally to this manuscript

[@] corresponding author: spncrfx@gmail.com

Abstract

Background: The southern United States (US) may be vulnerable to outbreaks of Zika Virus (ZIKV), given its broad distribution of ZIKV vector species and periodic ZIKV introductions by travelers returning from affected regions. As cases mount within the US, policymakers seek early and accurate indicators of self-sustaining local transmission to inform intervention efforts. However, given ZIKV's low reporting rates and geographic variability in both importations and transmission potential, a small cluster of reported cases may reflect diverse scenarios, ranging from multiple self-limiting but independent introductions to a self-sustaining local outbreak.

Methods and Findings: We developed a stochastic model that captures variation and uncertainty in ZIKV case reporting, importations, and transmission, and applied it to assess county-level risk throughout the state of Texas. For each of the 254 counties, we identified surveillance triggers (i.e., cumulative reported case thresholds) that robustly indicate further epidemic expansion. Regions of greatest risk for sustained ZIKV transmission include 33 Texas counties along the Texas-Mexico border, in the Houston Metro Area, and throughout the I-35 Corridor from San Antonio to Waco. Across this region, variation in reporting rates, ZIKV introductions, and vector habitat suitability drives variation in the recommended surveillance triggers for public health response. For high risk Texas counties, we found that, for a reporting rate of 20%, a trigger of two cumulative reported cases corresponds to a 60% chance of an ongoing local transmission.

Conclusions: With reliable estimates of key epidemiological parameters, including reporting rates and vector abundance, this framework can help optimize the timing and spatial allocation of public health resources to fight ZIKV in the US.

Introduction

In February 2016, Zika virus (ZIKV) was declared a public health emergency of international concern [1]. As of 11 May of 2016, the World Health Organization (WHO) confirmed mosquito-transmitted cases in 58 countries, with an estimated 290,000 cases in the Americas alone [2]. In the US, one of the primary vectors for ZIKV, *Aedes aegypti*, is thought to inhabit at least 30 states [3]. Texas ranks among the most vulnerable states for ZIKV transmission due to its suitable climate, international airports, and geographical proximity to affected countries [3–8]. Of the 503 imported ZIKV cases in the US, 35 have occurred in Texas. While these importations have yet to spark autochthonous (local) transmission, Texas has historically sustained several autochthonous outbreaks of one other arbovirus vectored by *Ae. Aegypti*—dengue (DENV) [9].

As peak mosquito season approaches in the US and more cases are potentially introduced via international travelers attending the Rio 2016 Olympic Games, public health decision makers will face considerable uncertainty in gauging the severity of the threat and in effectively initiating interventions, given the large fraction of unreported ZIKV cases as well as the shifting economic balance between intervention expenditure and disease burden [10,11]. Depending on the ZIKV symptomatic fraction, reliability and rapidity of diagnostics, importation rate, and transmission rate, the detection of five cases in a single Texas county, for example, may indicate five unrelated importations, a small outbreak from a single importation, or even a large, hidden epidemic underway (Fig 1). These possibilities are illustrated by prior outbreaks. In French Polynesia, a handful of suspected ZIKV cases were reported by October 2013; two months later an estimated 14,000-29,000 individuals had been infected [12,13]. By contrast, in Dominica, despite 18 confirmed cases in early 2016, two months later no sustained epidemic has yet ensued [14].

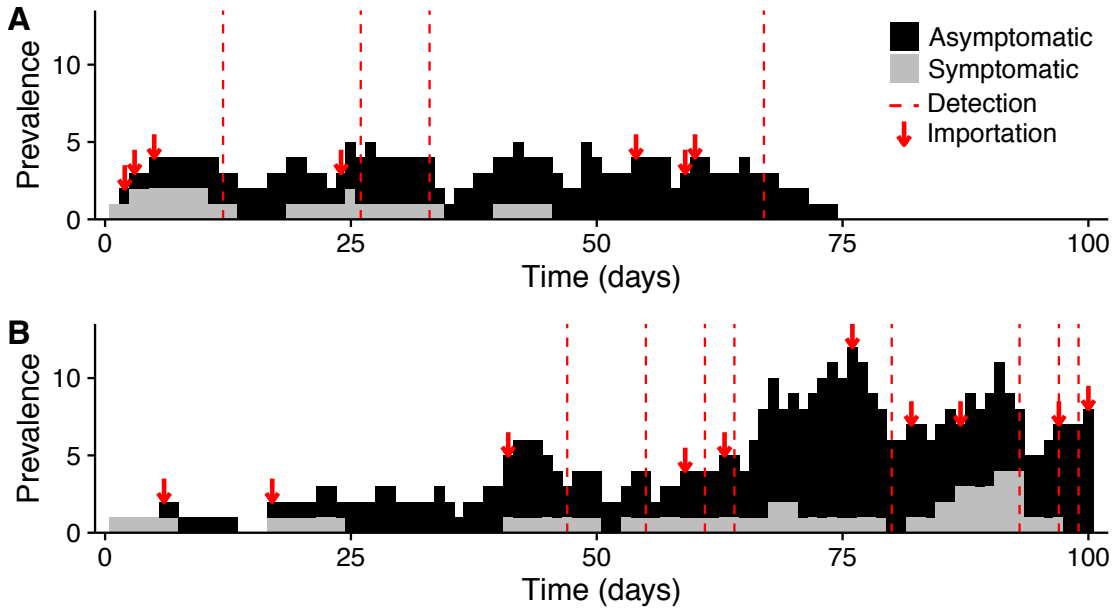

Fig 1. ZIKV emergence scenarios. A ZIKV infection could spark **(A)** a small self-limiting outbreak or **(B)** a full-blown epidemic**.** Cases are partitioned into symptomatic (grey) and asymptomatic (black). Arrows indicate new ZIKV importations by infected travelers and vertical dashed lines indicate case reporting events. On the 75th day, these divergent scenarios are almost indistinguishable to public health surveillance, as exactly four cases have been detected in both. By the 75th day, the outbreak (A) has died out while the epidemic (B) continues to grow. Each scenario is a single stochastic realization of the model with R_0=1.1, reporting rate of 10%, and introduction rate of 0.1 case/day.

Here, we develop a model to support real-time ZIKV risk assessment that accounts for uncertainty regarding ZIKV epidemiology, including importation rates, reporting rates, and local vector population density. This framework can be readily updated as our understanding of ZIKV evolves to provide actionable guidance for public health officials, in the form of surveillance triggers that robustly indicate imminent epidemic growth. By simulating ZIKV transmission using a stochastic branching process model [15] based on recent ZIKV data and epidemiological estimates, we derive thresholds of reported cases indicative of ongoing local transmission for each of the 254 counties in Texas. Our results suggest that counties along the Texas-Mexico border, in the Houston Metro Area, and throughout the I-35 Corridor from San Antonio to Waco are at highest risk for sustained outbreaks.

Methods

Model

To transmit ZIKV, a mosquito must bite an infected human, the mosquito must get infected with the virus, and then the infected mosquito must bite a susceptible human. Rather than explicitly model the full transmission cycle, we aggregate the two-part cycle of ZIKV transmission (mosquito-to-human and human-to-mosquito) into a single meta-latent period, and do not explicitly model mosquitos. For the purposes of this study, we need only ensure that the model produces a realistic human-to-human generation time of ZIKV transmission.

We simulate a Susceptible-Exposed-Infectious-Recovered (SEIR) transmission process stemming from a single ZIKV infection using a Markov branching process model, stratifying for reported and unreported cases. The temporal evolution of the compartments is governed by daily probabilities for infected individuals transitioning between E, I and R states, new ZIKV introductions, and reporting of current infectious cases (Table S7). We assume that infectious cases cause a Poisson distributed number of secondary cases per day (via human to mosquito to human transmission), and that low reporting rates correspond to the percentage (~20%) of symptomatic ZIKV infections [10]. We make the simplifying assumption that asymptomatic cases transmit ZIKV at the same rate as symptomatic cases, which can be modified if future evidence suggests otherwise.

Serial interval

The ZIKV serial interval measures the average duration from an exposure to the subsequent exposure of a secondary case, and is estimated to range from 10 to 23 days [16]. Using boxcar models [17] for both the infectious and meta-latent period, we chose model parameters that produce a comparable delay between subsequent human infections rather than fit a more mechanistic model of human and vector infection and latency to ZIKV case data. First, we

solved for transition rates that yield a negative binomial distribution of infectious periods with mean duration of 9.88 days (Table S6) [18]. Then, we fit the meta-latent period so that the combined duration of the infectious and meta-latent periods matched the empirical ZIKV serial interval distribution [16], yielding a mean meta-latent period of 10.4 days (95% CI 6-17) and a mean serial interval of 15.3 days (95% CI 9.5-23.5). Given that the meta-latent period includes human and mosquito incubation periods and mosquito biting rates, this range is consistent with the estimated 5.9 day human ZIKV incubation period [18]. This flexible framework can be extended and updated readily as we learn more about ZIKV.

Importation rate

Our analysis assumes that any ZIKV outbreaks in Texas will originate with infected travelers returning from regions with high ZIKV activity. During the first quarter of 2016, 27 travel-associated cases of ZIKV were reported in Texas, with 11 occurring in Houston's Harris County [19], yielding a baseline first quarter estimate of 0.3 imported cases per day throughout Texas. Given the geographic and biological overlap between ZIKV, DENV and Chikungunya (CHIKV), we use historical DENV and CHIKV importation data to inform our importation model, while recognizing that future ZIKV importations may be fueled by large epidemic waves in neighboring regions and travel from the 2016 Olympics, and thus far exceed recent DENV and CHIKV importations [20]. In 2014 and 2015, arbovirus introductions into Texas were threefold higher during the third quarter than the first quarter of each year, perhaps driven by seasonal increases in arbovirus activity in endemic regions and the approximately 40% increase in international travel to the US [21]. Taking this as a *baseline* (lower bound) scenario, we project a corresponding increase in ZIKV importations to 0.9 cases per day (statewide) for the third quarter. We also consider an *elevated* importation scenario, in which the first quarter cases (27) in Texas represent only the symptomatic (20%) imported cases, corresponding to a projected third quarter importation rate of 4.5 cases/day.

149 To estimate the importation rate for a specific county, we multiply the statewide rate by
150 the county importation probability, which is given by a maximum entropy model [22] that we fit
151 to the 183 DENV, 38 CHIKV, and 31 ZIKV reported Texas importations from 2002 to 2016.
152 DENV, CHIKV, and ZIKV importation patterns differ most noticeably along the Texas-Mexico
153 border. Endemic DENV transmission and sporadic CHIKV outbreaks in Mexico regularly spill
154 over into neighboring Texas counties. In contrast, ZIKV is not yet as widespread in Mexico as it
155 is in Central and South America, with no reported ZIKV importations along the border to date.
156 We included DENV and CHIKV importation data in the model fitting so as to consider potential
157 future importations pressure from Mexico, as ZIKV continues its northward expansion. We
158 analyzed 72 socio-economic, environmental, and travel variables, and used both representative
159 variable selection [23] and predictive variable selection [24] to identify the most informative
160 variables. Near duplicate variables and those that contributed least to model performance, based
161 on out-of-sample cross validation, were discarded, reducing the original set of 72 variables to 10
162 (Supplement §1).
163
164 Estimating local transmission rates
165 Upon ZIKV importation by an infected traveler, the risk of ZIKV emergence will depend
166 on the likelihood of mosquito-borne transmission. For each Texas county, we used the Ross-
167 Macdonald formulation to estimate the ZIKV reproduction number (R_0), which is the average
168 number of secondary infections caused by the introduction of a single infectious individual into a
169 fully susceptible population (Supplement §2) [25]. To parameterize the model, we use mosquito
170 life history estimates from a combination of DENV and ZIKV studies and estimated *Aedes*
171 *aegypti* abundance for each county [4]. For parameters that are sensitive to temperature (i.e.,
172 mosquito mortality and the extrinsic incubation period), we adjusted the estimates using average

173 reported temperatures for the month of August [26]. We then obtained the county-level ZIKV
174 transmission rate, using $\beta = R_0 * \gamma$.

175

176 Identifying Surveillance Triggers

177 Policymakers must often make decisions in the face of uncertainty, such as when and
178 where to initiate ZIKV interventions. Our stochastic framework allows us to address a simple but
179 important question: *at what point (after how many reported cases), has the probability of ongoing*
180 *local transmission reached a critical threshold*. The choice of critical threshold will depend on
181 the risk tolerance of the policymaker. A policymaker wishing to trigger interventions early, upon
182 even a low probability of epidemic spread, has a low tolerance for failing to intervene (false
183 negative); a policymaker willing to wait longer, has a higher risk tolerance.

184 For each scenario, we ran 10,000 stochastic simulations, which terminate when the
185 outbreak ceases or cumulative infections reaches 2,000. We classify simulations as either
186 epidemics or self-limiting outbreaks; epidemics are those reaching 2,000 cumulative infections
187 with a maximum prevalence above 50 (Fig S3). We define prevalence as the number of current
188 unreported and reported infections. To identify surveillance triggers, we solved for the minimum
189 number of cumulative reported cases (c) that indicate future epidemic expansion with a specified
190 probability (p). That is, we find c such that among all simulations that eventually reach c, at least
191 a fraction p subsequently progress into an epidemic. For example, if we set our threshold
192 probability (risk tolerance) to p=0.5 and derive an epidemic trigger of c=10 reported cases, then
193 we expect outbreaks that reach 10 reported cases to have a 50% chance of future epidemic
194 expansion. In supplementary analysis, we also consider surveillance triggers for detecting when
195 the current prevalence has reached a specified threshold (Fig S6).

196

197 *Uncertainty Analysis*

198 Given the considerable uncertainty regarding ZIKV epidemiology, we solve for
199 surveillance triggers assuming that both R_0 and importation rate are unknown, but lie within a
200 plausible range for Texas. We consider two scenarios: a *high risk* scenario, where R_0 is thought to
201 exceed one, and a completely *unknown* risk scenario (Fig S5). For each case, we derive triggers
202 by randomly drawing 10,000 simulations from all combinations of Texas (baseline) importation
203 and transmission rates from either the high risk Texas counties ($R_0 \geq 1$) or all counties.
204
205 **Results**
206 To develop surveillance triggers for Texas, we first project county-level ZIKV
207 importation and transmission rates for August 2016. ZIKV importation risk within Texas is
208 predicted by variables reflecting urbanization, mobility patterns, and socioeconomic status (Table
209 S4), and is concentrated in metropolitan counties of Texas (Fig 2A). The highest risk counties,
210 Harris (with an estimated 27% chance of receiving the next imported Texas case) and Travis
211 (10%), which includes Austin, both contain international airports. Other high risk regions include
212 Brazos County, the Dallas and San Antonio metropolitan areas, and several counties along the
213 Texas-Mexico border.
214 We also estimate county-level ZIKV risks of autochthonous ZIKV transmission (Fig 2B),
215 and find that the majority of Texas counties (87%) have an estimated $R_0<1$, and thus are unlikely
216 to sustain local epidemics. The Southeast region of Texas has the highest estimated transmission
217 risk, driven primarily by high mosquito habitat suitability. These estimates are sensitive to
218 uncertainty in several parameters (Fig S1-S2), and should be updated as we learn more about
219 ZIKV. Without perfect estimates for county R_0, we develop plausible distributions for a county of
220 high or unknown risk for local transmission using our 254 county estimates, resulting in a median
221 high risk R_0 of 1.1 (95% CI: 1.0-1.8) and median unknown risk R_0 of 0.5 (95% CI: 0.0-1.2).
222

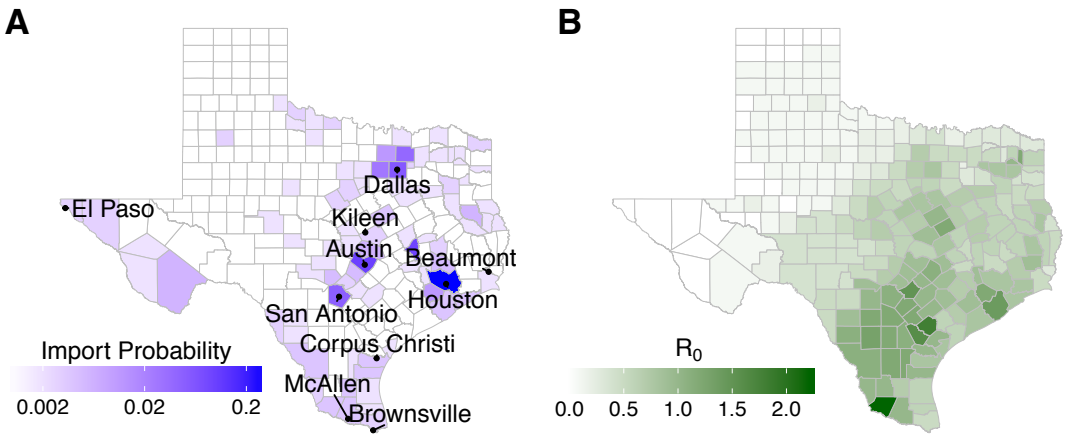

Fig 2. ZIKV importation and transmission risk across Texas. (A) Color shading indicates the probability that the next ZIKV import will occur in a given county for each of the 254 Texas counties. Probability is colored on a log scale. The 10 most populous cities in Texas are labeled. Houston's Harris County has 2.7 times greater chance than Austin's Travis County of receiving the next imported case. **(B)** Estimated county-level R_0 for ZIKV.

Under a single set of epidemiological conditions, wide ranges of outbreaks are possible (Fig 3A). The relationship between what policymakers can observe (cumulative reported cases) and what they wish to know (current prevalence) can be obscured by such uncertainty, and will depend critically on both the transmission and reporting rates (Fig 3B). If key drivers, such as R_0, can be estimated with confidence, then the breadth of possibilities narrows, enabling more precise surveillance. For example, under a known moderate R_0 scenario, ten cumulative reported cases corresponds to an expected prevalence of 6 with a 95% CI of 1-15; under an unknown high R_0 scenario, the same number of cases corresponds to an expected prevalence of 10 with a much wider 95% CI of 2-33 (Fig 3B).

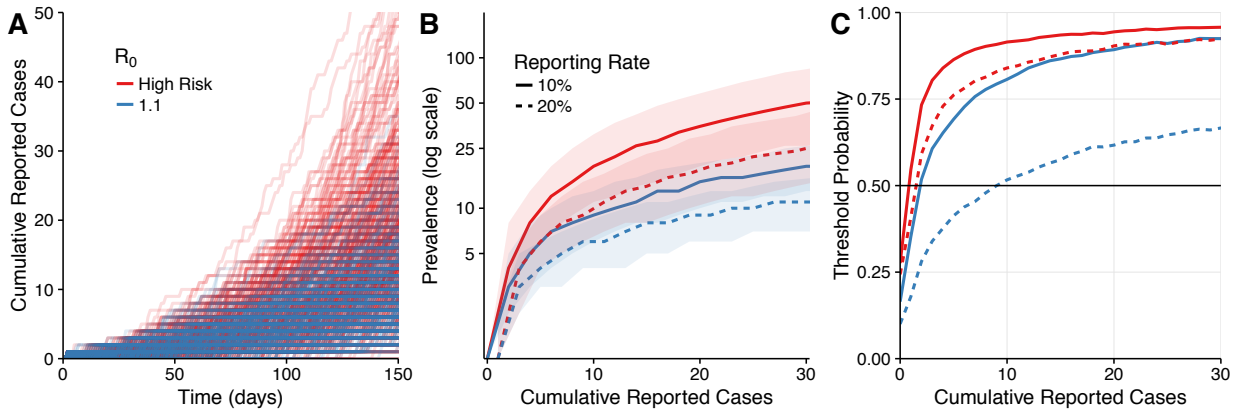

Fig 3. Surveillance triggers for detecting and forecasting ZIKV transmission. (A) Simulated outbreaks, assuming an importation rate of 0.01 case per day, for a known (moderate risk) R_0 (blue) or an unknown high risk R_0 (red). 2,000 randomly sampled simulations are shown for each scenario. (B) Current prevalence as a function of the cumulative detected cases, assuming an importation rate of 0.01 case per day, for a known R_0 (blue) or an unknown high-risk R_0 (red), and a relatively high (dashed) or low (solid) reporting rate. Ribbons indicate 50% quantiles. (C) The increasing probability of imminent epidemic expansion across a range of reported cases, compared across the high risk (red) and known moderate risk (blue) for a low (solid) and high (dashed) reporting rate. Suppose cases arise in a known high risk county and a policymaker wishes to trigger a response as soon as the chance of sustained transmission reaches 50% (horizontal line). Then, if the reporting rate is 20%, he or she should trigger the response as soon as the 2nd case is reported.

We apply our model to address the question, *at what point (after how many reported cases), has the probability of ongoing local transmission reached a critical threshold*. Under both a known moderate risk and unknown high risk scenario, we track the probability of epidemic expansion following each additional reported case (Fig 3C). Across the full range of reported cases, the probability of epidemic spread will always be higher under the high risk scenario, with the moderate risk scenario showing more sensitivity to the reporting rate. These curves can support both real-time risk assessment as cases accumulate and the identification of surveillance triggers indicating when risk exceeds a specified threshold. For example, suppose a policymaker

263 wishes to initiate an intervention when the chance of sustained transmission exceeds 50%. In the
264 high risk scenario, they should act immediately following the 2nd or 3rd reported case; in the
265 moderate risk scenario, the corresponding trigger rangers from 3 to 10 reported cases, depending
266 on the reporting rate. As the policymaker's threshold (risk tolerance) increases, the recommended
267 surveillance triggers can increase by orders of magnitude.

268 We determine county-level surveillance triggers throughout Texas, assuming that a
269 policymaker would act when the probability of sustained local transmission reaches 70%, under
270 two importation scenarios: (1) a baseline importation rate extrapolated from recent importations
271 to August 2016 (Fig 4A), and (2) an elevated importation scenario assuming that only one fifth of
272 ZIKV importations (the symptomatic proportion) have been observed (Fig 4B). Under baseline
273 importations, only 21 of the 254 counties in Texas are expected to attain the trigger conditions
274 (Fig 4A), and have triggers ranging from 1 (Starr County) to 71 (Bastrop County) reported cases,
275 with a mean of 15. The San Antonio metropolitan region appears to be most at risk, with almost
276 every county capable of epidemics and triggers ranging from 2 to 5 reported cases. The greater
277 Houston metropolitan area also is at high risk, with surveillance triggers of 2 (Brazoria) and 3
278 (Fort Bend) cases.

279 Under the elevated importation rate scenario, the mean surveillance triggers decrease by
280 4 reported cases (Fig 4B) and the size of Texas' population at risk for sustained ZIKV
281 transmission is expected to increase from ~14% to ~30%. If the importation rate is sufficiently
282 high, even lower risk regions (R_0 just below one) can experience sustained outbreaks. For
283 example, under the elevated importation scenario, Harris county, with an estimated $R_0 = 0.8$, is
284 likely to suffer persistent transmission, fueled by an expected 1.2 importations per day. Notably,
285 the Dallas metropolitan area is projected to be at minimal risk for sustained transmission under
286 both scenarios.

287 To avoid confusion and facilitate implementation, policymakers may wish to issue
288 common guidelines for all counties. For example, they may seek a common surveillance trigger

289 that provides robust warning across the plausible range of local conditions. For example,
290 assuming a 20% reporting rate, we consider the implications of a statewide trigger of two
291 reported cases (Fig 4C). Upon seeing two cases, the epidemic risk varies widely, with most
292 counties having near zero probabilities of a sustained outbreak and a few counties far exceeding
293 50%. For example, two reported cases in Starr County, along the Texas-Mexico border,
294 correspond to a 98% chance of ongoing transmission.

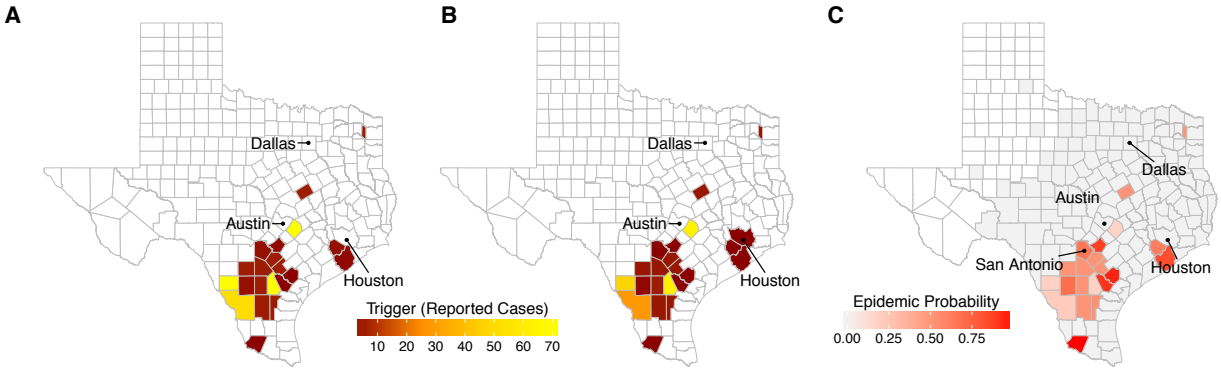

295

296 **Fig 4. ZIKV surveillance triggers across Texas.** Recommended county-level surveillance triggers for detecting that
297 the probability of sustained local transmission has reached p_T=0.70, assuming a reporting rate of 20%. These reflect **(A)**
298 the baseline importation scenario for August 2016 (81 cases statewide per 90 days) projected from historical arbovirus
299 data, and **(B)** the elevated importation scenario (405 cases statewide per 90 days) that assumes recent ZIKV
300 importations represent only 20% of all importations. White counties indicate that less than 1% of the 10,000 simulated
301 outbreaks resulted in sustained transmission. **(C)** Assuming the baseline importation scenario, the probability of an
302 impending epidemic at the moment the second ZIKV case is reported in a county. White counties never reach two
303 reported cases, across all 10,000 simulated outbreaks; light gray counties reach two cases, but never experience
304 epidemics.

305

306 **Discussion**

307 US public health authorities are responding to ZIKV importations and preparing for the
308 possibility of ZIKV outbreaks in vulnerable regions. A key challenge is knowing when and where
309 to initiate interventions based on potentially sparse and biased ZIKV case reports. Our simple
310 model is designed to address this challenge by developing robust surveillance triggers for

311 epidemic events, such as reaching a threshold of current ZIKV infections indicative of future
312 epidemic expansion. We demonstrate its application across the 254 ecologically and
313 demographically diverse counties of Texas, a high risk state [5,6,8]. Based on county-level
314 estimates for ZIKV importation and transmission rates (Fig 3) we expect that most Texas counties
315 are not at risk for a sustained ZIKV epidemic (Fig 4A). However, 30% of Texas' population
316 resides in vulnerable regions, including the cities of Austin, San Antonio, and Waco along the I-
317 35 corridor, Houston, and the Rio Grande Valley. The higher the ZIKV importation rate in these
318 locations, the higher the chance of sustained transmission (Fig 4B). However, even in the most
319 high risk regions of Texas, we expect far more limited ZIKV transmission than observed in
320 Central America, South America, and Puerto Rico, where R_0 has been estimated to be as high as
321 11 [25,27,28]. This is consistent with recent introductions of DENV and CHIKV into Texas,
322 which have failed to spark large epidemics.

323 As an example, we suppose that a policymaker wishes to initiate interventions upon the
324 epidemic probability reaching 70%. The recommended triggers range from 1 to 71 reported cases,
325 across the 21 Texas counties capable of sustaining such outbreaks. The model can also be used to
326 assess universal triggers intended to robustly detect sustained transmission across a range of local
327 conditions. A risk averse policymaker will likely select a very low trigger, ensuring early
328 detection in the riskiest sites at the cost of false alarms in low risk locations (Fig 4C). Note that
329 our triggers include all imported and locally transmitted cases; trigger specificity may be
330 improved by rapidly and accurately excluding imported cases from the count and restarting the
331 count upon sufficient temporal separation of cases.

332 In Texas' vulnerable regions, where the estimated reproduction numbers lie above one,
333 frequent importations can compound the epidemic risk. Additionally, importations in counties
334 where estimated reproductive numbers lie below one, like Harris, can spark substantial
335 transmission (Fig 4B). These findings apply only to the early, pre-epidemic phase of ZIKV in
336 Texas, when travel from affected regions outside the contiguous US is the primary importation

337 source. If self-sustaining outbreaks emerge within Texas, there would likely be county-to-county
338 importations that are not yet included in the model, and could increase risk in counties
339 surrounding high risk regions.

340 Importantly, our analyses rest on the very recent and limited scientific investigations of
341 ZIKV's biology and epidemiology, and should be continually updated as our understanding
342 matures. Furthermore, while we demonstrated triggers for a few plausible scenarios, the design of
343 a trigger--both the event to be detected and the probability threshold upon which to take action--
344 requires extensive public health expertise and deliberation. Nonetheless, this simple framework
345 offers a flexible means for bringing current data and expert knowledge to assist critical public
346 health decision making.

347 The reporting rate dictates the relationship between observed cases and the underlying
348 outbreak, and its magnitude impacts the timeliness and precision of detection. If only a small
349 fraction of cases are reported, the first few reported cases may correspond to a wide range of
350 underlying epidemiological conditions, from isolated introductions to a growing epidemic. In
351 contrast, if most cases are reported, policymakers can wait longer (in terms of the number of
352 detected cases) to trigger interventions and have more confidence in their epidemiological
353 assessments. ZIKV reporting rates are expected to remain quite low, because an estimated 80% of
354 infections are asymptomatic, and DENV reporting rates have historically matched its
355 asymptomatic proportion [10,29]. Obtaining a realistic estimate of the ZIKV reporting rate is
356 arguably as important as increasing the rate itself, with respect to reliable situational awareness
357 and forecasting. An estimated 8-22% of ZIKV infections were reported during the 2013-2014
358 outbreak in French Polynesia [28]; similarly, an estimated 10% have been reported during the
359 ongoing epidemic in Columbia [27]. While these provide a baseline estimate for the US, there are
360 many factors that could increase (or decrease) the detection rate, such as ZIKV awareness among
361 both the public and health-care practitioners. Thus, rapid estimation of the reporting rate should
362 be a high priority. While some methods require extensive epidemiological data not typically

available early in an outbreak [30], a new method exploiting early outbreak viral sequence data was introduced during the recent West African Ebola epidemic [31]. However, as of May 2016, there are no US ZIKV sequences available on GenBank and few available from other regions.

Our flexible framework can help policymakers make sound risk assessments from noisy and biased surveillance data. It forces analysts to be explicit about risk tolerance, that is, the certainty needed before sounding an alarm. For example, should ZIKV-related pregnancy advisories be issued when there is only 5% chance of an impending epidemic? 10% chance? 80%? A policymaker has to weigh the costs of false positives--resulting in unnecessary fear and/or intervention--and false negatives--resulting in suboptimal disease control and prevention--complicated by the difficulty inherent in distinguishing a false positive from a successful intervention. The more risk averse the policymaker (with respect to false negatives), the earlier the trigger should be, which can be exacerbated by low reporting rates, high importation rate, and inherent ZIKV transmission potential. In ZIKV prone regions with low reporting rates, even risk tolerant policymakers should act quickly upon seeing initial cases; in lower risk regions, longer waiting periods may be prudent.

Acknowledgements

We acknowledge the Texas Advanced Computing Center (TACC) at The University of Texas at Austin for providing High performance computing resources that have contributed to the research results reported within this paper. URL: http://www.tacc.utexas.edu.

References

1. Gulland A. Zika virus is a global public health emergency, declares WHO. BMJ. BMJ Publishing Group Ltd; 2016;352. doi:10.1136/bmj.i657
2. World Health Organization. Zika situation report: 12 May 2016 [Internet]. 2016. Available: http://www.who.int/emergencies/zika-virus/situation-report/12-may-2016/en/

389 3. About estimated range of Aedes aegypti and Aedes albopictus in the United States, 2016
390 Maps. Centers for Disease Control and Prevention [Internet]. Available:
391 http://www.cdc.gov/zika/vector/range.html
392 4. Kraemer MUG, Sinka ME, Duda KA, Mylne A, Shearer FM, Barker CM, et al. The global
393 distribution of the arbovirus vectors Aedes aegypti and Ae. albopictus. Elife. eLife
394 Sciences Publications Limited; 2015;4: e08347. Available:
395 http://elifesciences.org/content/4/e08347v3
396 5. Messina JP, Kraemer MU, Brady OJ, Pigott DM, Shearer FM, Weiss DJ, et al. Mapping
397 global environmental suitability for Zika virus. Elife. eLife Sciences Publications Limited;
398 2016;5: e15272. Available: https://elifesciences.org/content/5/e15272
399 6. Gardner LM, Chen N, Sarkar S. Global risk of Zika virus depends critically on vector
400 status of Aedes albopictus. Lancet Infect Dis. Elsevier; 2016;16: 522–523. Available:
401 http://www.thelancet.com/article/S1473309916001766/fulltext
402 7. Peterson AT, Osorio J, Qiao H, Escobar LE. Zika virus, elevation, and transmission risk.
403 PLoS Curr Outbreaks. 2016;9.
404 doi:10.1371/currents.outbreaks.a832cf06c4bf89fb2e15cb29d374f9de
405 8. Monaghan AJ, Morin CW, Steinhoff DF, Wilhelmi O, Hayden M, Quattrochi DA, et al.
406 On the Seasonal Occurrence and Abundance of the Zika Virus Vector Mosquito Aedes
407 Aegypti in the Contiguous United States. PLoS Curr. 2016; 1–31.
408 doi:10.1371/currents.outbreaks.50dfc7f46798675fc63e7d7da563da76
409 9. Arbovirus Activity in Texas 2014 Surveillance Report.
410 10. Duffy M. Chen T.Hancock T. Powers A. Kool J. Lanciotti R. Pretrick M. Zika Virus
411 Outbreak on Yap Island, Federated States of Micronesia. N Engl J Med. 2009;360: 2536–
412 2543.
413 11. Alfaro-Murillo JA, Parpia AS, Fitzpatrick MC, Tamagnan JA, Medlock J, Ndeffo-Mbah
414 ML, et al. A Cost-Effectiveness Tool for Informing Policies on Zika Virus Control. PLoS

415 Negl Trop Dis. Public Library of Science; 2016;10: e0004743. Available:
416 http://journals.plos.org/plosntds/article?id=10.1371/journal.pntd.0004743
417 12. Sudre B, Danielsson N, Rakotoarivony LM, Bortel W Van, Zeller H, Jansa J. Zika virus
418 infecton outbreak French Polynesia. 2014; 1–12.
419 13. Cao-Lormeau V-M, Roche C, Teissier A, Robin E, Berry A-L, Mallet H-P, et al. Zika
420 Virus, French Polynesia, South Pacific, 2013. Emerg Infect Dis J. 2014;20: 1084.
421 doi:10.3201/eid2006.140138
422 14. Pan American Health Organization, World Health Organization. Cumulative Zika
423 suspected and confirmed cases reported by countries and territories in the Americas, 2015-
424 2016 [Internet]. Washington, D.C.; 2016. Available:
425 http://ais.paho.org/phip/viz/ed_zika_cases.asp
426 15. Getz WM, Lloyd-Smith JO. Basic methods for modeling the invasion and spread of
427 contagious diseases. Dis Evol Model concepts, data Anal AMS-DIMACS Ser. 2006;71:
428 87.
429 16. Majumder MS, Cohn E, Fish D, Brownstein JS. Estimating a feasible serial interval range
430 for Zika fever. Bull World Health Organ. 2016;
431 17. Lloyd AL. Realistic Distributions of Infectious Periods in Epidemic Models: Changing
432 Patterns of Persistence and Dynamics. Theor Popul Biol. 2001;60: 59–71.
433 doi:10.1006/tpbi.2001.1525
434 18. Lessler J, Ott CT, Carcelen AC, Konikoff JM, Williamson J, Bi Q, et al. Times to Key
435 Events in the Course of Zika Infection and their Implications for Surveillance: A
436 Systematic Review and Pooled Analysis. bioRxiv. 2016; Available:
437 http://biorxiv.org/content/early/2016/03/02/041913.abstract
438 19. "Texas Department of State Health and Human Services." Zika in Texas [Internet]. 2016
439 [cited 5 Apr 2016]. Available: http://www.texaszika.org/
440 20. Musso D, Cao-Lormeau VM, Gubler DJ. Zika virus: following the path of dengue and

chikungunya? Lancet (London, England). Elsevier; 2015;386: 243–4. Available: http://www.thelancet.com/article/S0140673615612739/fulltext

21. Office of Travel & Tourism Industries. US Monthly Arrivals Trend Line [Internet]. 2014 [cited 25 May 2016]. Available: http://travel.trade.gov/view/m-2014-I-001/index.html

22. Jaynes ET. Information Theory and Statistical Mechanics. Phys Rev. American Physical Society; 1957;106: 620–630. doi:10.1103/PhysRev.106.620

23. Wolsey LA. Integer programming. Vol. 42. New York: Wiley New York; 1998.

24. Merow C, Smith MJ, Silander JA. A practical guide to MaxEnt for modeling species' distributions: what it does, and why inputs and settings matter. Ecography (Cop). Blackwell Publishing Ltd; 2013;36: 1058–1069. doi:10.1111/j.1600-0587.2013.07872.x

25. Perkins A, Siraj A, Warren Ruktanonchai C, Kraemer M, Tatem A. Model-based projections of Zika virus infections in childbearing women in the Americas. 2016; doi:10.1101/039610

26. World Media Group L. USA.com: Texas [Internet]. [cited 25 May 2016]. Available: http://www.usa.com/texas-state.htm

27. Rojas DP, Dean NE, Yang Y, Kenah E, Quintero J, Tomasi S, et al. The Epidemiology and Transmissibility of Zika Virus in Girardot and San Andres Island, Colombia. bioRxiv. 2016; Available: http://biorxiv.org/content/early/2016/04/24/049957.abstract

28. Kucharski AJ, Funk S, Eggo RM, Mallet H, Edmunds WJ, Nilles EJ. Transmission dynamics of Zika virus in island populations : a modelling analysis of the 2013 – 14 French Polynesia outbreak. bioRxiv. 2016; 1–15.

29. Dechant E, Rigau-Perez J. Hospitalizations for suspected dengue in Puerto Rico, 1991-1995: estimation by capture-recapture methods. The Puerto Rico Association of Epidemiologists. Am J Trop Med Hyg. 1999;61: 574–578. Available: http://www.ajtmh.org/content/61/4/574.short

30. Bhatt S, Gething PW, Brady OJ, Messina JP, Farlow AW, Moyes CL, et al. The global

467 distribution and burden of dengue. Nature. Nature Publishing Group; 2013;496: 504–507.
468 doi:10.1038/nature12060
469 31. Scarpino S V, Iamarino A, Wells C, Yamin D, Ndeffo-Mbah M, Wenzel NS, et al.
470 Epidemiological and viral genomic sequence analysis of the 2014 ebola outbreak reveals
471 clustered transmission. Clin Infect Dis. Oxford University Press; 2015;60: 1079–82.
472 Available: http://cid.oxfordjournals.org/content/early/2015/01/05/cid.ciu1131.full
473
474